Nanoscale phase separation in quasi-uniaxial and biaxial strained multiferroic thin films

Yajun Qi,[1,2,3] Chuanwei Huang,[1] Zuhuang Chen,[1] Zhenlin Luo,[4] Yiqian Wang,[5] Jun Guo,[1] Tim White,[1] Junling Wang,[1] Chen Gao,[4] Thirumany Sritharan,[1] and Lang Chen[1,3,a)]

[1]*School of Materials Science and Engineering, Nanyang Technological University, Singapore 639798, Singapore*

[2]*Department of Materials Science and Engineering, Hubei University, Wuhan 430062, People's Republic of China*

[3]*Energy Research Institute @ NTU (ERI@N), Research Techno Plaza, 5th Storey, 50 Nanyang Drive, Singapore 637553*

[4]*National Synchrotron Radiation Laboratory, University of Science and Technology of China, Hefei 230029, People's Republic of China*

[5]*The Cultivation Base for State Key Laboratory, Qingdao University, Qingdao 266071, People's Republic of China*

(Received 21 April 2011; accepted 9 September 2011; published online 29 September 2011)

Nanoscale phase separation was investigated in epitaxial strained $BiFeO_3$ thin films on $LaAlO_3$ single crystal substrate. In biaxial strained thin films, nanoscale mixtures of the tetragonal-like and rhombohedral-like phases occur with a film thickness above 35 nm. For 10-30 nm ultrathin ones, tetragonal-like single phase is confirmed using synchrotron x-ray and the atomic force microscopy studies. However, nanoscale phase separations are still observed in quasi-uniaxial transmission electron microscopy foil specimens for those ultrathin films, indicating the phase separation emerges in a much smaller thickness in uniaxial constraint films than that in biaxial ones. © *2011 American Institute of Physics*. [doi:10.1063/1.3644958]

Recently, a biaxial strain-driven phase separation in multiferroic $BiFeO_3$ (BFO) epitaxial thin films has attracted great attentions due to its huge potentials on data storage, sensor, and actuator applications.[1–6] This phase separation gives rise to a strain-induced morphotropic phase boundary-like behavior and results in large piezoelectric responses.[1,3] Previous studies by atomic force microscopy (AFM) and x-ray diffraction (XRD) confirmed the coexistence of the tetragonal-like (T) and rhombohedral-like (R) phases in relatively thick BFO films grown on $LaAlO_3$ (LAO) and $LaSrAlO_4$ substrates[3–6] and suggested that the critical thickness for the appearance of the R-like phase on LAO is around 35 nm.[1] On the other hand, novel functionalities in advanced materials can be achieved by reducing the biaxial constrain to a uniaxial clamping condition.[7–9] For example, in MnAs films epitaxially grown on GaAs substrate, the temperature dependant phase separation and phase volume fraction evolution between hexagonal and orthorhombic phases were totally different under uniaxial and biaxial constraints.[7] The substrate-induced uniaxial strain in VO_2 nanobeams changes the relative stability of the metal (M) and insulator (I) phases and leads to spontaneous formation of periodic, alternating M-I domain patterns during the M-I transition.[8] In this letter, we aim to clarify the nanoscale phase separation in strained epitaxial BFO thin films with biaxial and uniaxial constraints using transmission electron microscopy (TEM) with the aid of AFM and XRD. For the quasi-uniaxial TEM foil specimens, the nanoscale phase separations were even observed in a 12 nm-thick ultrathin sample.

BFO thin films with several thicknesses between 10 and 80 nm were deposited on (001) LAO single crystal substrates by pulsed laser deposition. Details of the deposition procedure and AFM as well as synchrotron X-ray Reciprocal Space Maps (RSM) investigations are described elsewhere.[4,6] Cross-sectional TEM specimens were prepared using the standard procedure consisting of cutting, gluing, mechanical polishing, and ion milling. The ion milling process was performed on Precision Ion Polishing System (PIPS, model 691, Gatan) with an incident ion angle of 5° and an accelerating voltage of 3 kV using liquid N_2 to cool the stage. TEM investigations were carried out on a JEOL JEM2100F (FEG) electron microscope operated at 200 kV.

Figure 1(a) shows characteristic AFM topography image of a ~10-nm-thick BFO film on LAO substrate. Atomically flat terraces with single-unit-cell-high steps appeared as periodic lines can be observed, confirming the high quality growth of the film. The root-mean-square roughness of the

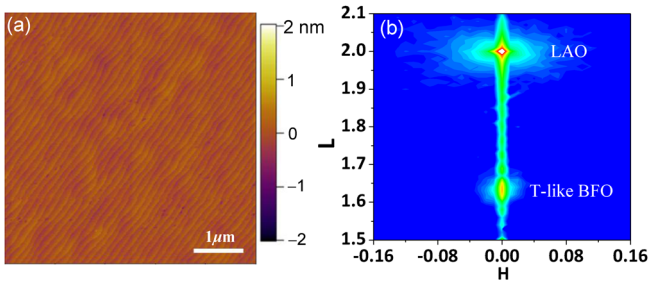

FIG. 1. (Color online) (a) AFM topography image of a ~10 nm-thick BFO film on a LAO substrate. (b) Synchrotron XRD RSM on (002) reflections of the 10 nm-thick BFO film. Two reflection spots arise from the substrate LAO (top) and BFO (bottom), respectively. The out-of-plane *c* lattice parameter is determined to be 4.64 Å, a typical value for the T-like phase of BFO.

a)Author to whom correspondence should be addressed. Electronic mail: langchen@ntu.edu.sg.

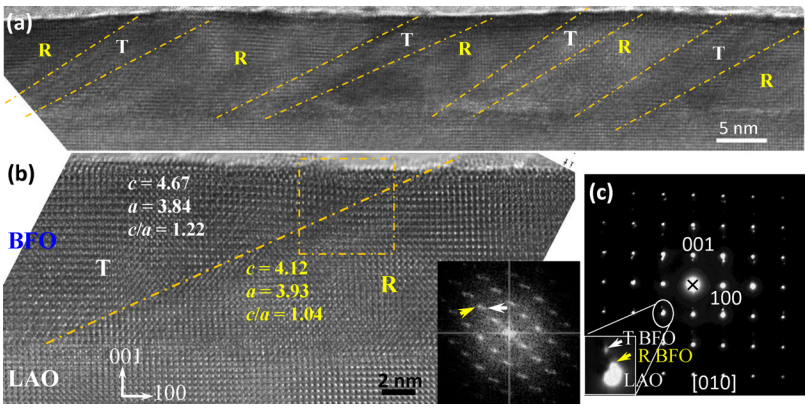

FIG. 2. (Color online) (a) and (b) Cross-sectional TEM images of the 12 nm BFO film. "T" and "R" denote the T-like and R-like phases, respectively. Inset of (b): FFT of the rectangle area in (b). (c) [010] zone axis SAED pattern taken from the BFO layer and the substrate LAO with the weak spots for BFO. The $(\bar{1}0\bar{1})$ reflection splitting into three spots was enlarged in the inset, corresponding to the reflections of T-like, R-like BFO and LAO from the top to the bottom, respectively.

film surface is 1.5 Å over a 5 μm × 5 μm scan area. No stripe contrast appears in all AFM topography images, indicating the single phase of the film.[1,5,6] The XRD investigation of the sample showed pure T-like phase structure in the film as shown in the RSM of Fig. 1(b). Only two reflection peaks, LAO (002) (top) and BFO (002) (bottom) were detected. The c lattice parameter of BFO film is computed to be ~4.64 Å, which is in agreement with values typically reported for this phase.[1]

Figure 2(a) shows the cross-sectional TEM image of a 12-nm-thick BFO film. A clear, planar interface is evident between the BFO film and the LAO substrate. Figure 2(c) illustrates the selected-area electron diffraction (SAED) pattern of an area including BFO and LAO, which is indexed on the basis of the pseudo-cubic unit cell. It is a superposition of [010] BFO and [010] LAO SAED patterns, which have the same [001] direction. Combining with the high-resolution TEM (HRTEM) image in Fig. 2(b), it reveals that the film is almost perfectly epitaxial with the substrate giving the orientation relationship as (001) BFO//(001) LAO and [010] BFO//[010] LAO. Furthermore, more than 30 HRTEM images along the interface at different spots show that the film is free of dislocations in a large area.

Producing a cross-sectional TEM specimen from a thin film-on-substrate sample would reduce the biaxial constraint that exists in the original sample to a quasi-uniaxial one. The results obtained by TEM investigations of the quasi-uniaxial TEM foil specimens however tend to reveal different structural information. A significant amount of R-like phase in the TEM specimen was detected although the film thickness is only 12 nm, in contradiction with the AFM and XRD investigations in a biaxial clamping case. As distinguished clearly in Figs. 2(a) and 2(b), the two phases are alternating in a R-T-R-T-R…. pattern. The lattice parameters measured from the high resolution image for each phase are the statistic results of more than 30 HRTEM images taken from different area using the LAO substrate as a calibration standard, as given in Fig. 2(b), which are in accordance with the results deduced from the SAED pattern. The T-like phase has a larger tetragonal ratio ($c/a = 1.22$) compared to the R-like phase (1.04). As shown in the inset of Fig. 2(c), the $(\bar{1}0\bar{1})$ reflection splits into three spots corresponding to T-like, R-like BFO and LAO, respectively. Furthermore, in the inset of Fig. 2(b), the fast Fourier transform (FFT) of the area marked by a rectangle in Fig. 2(b) also shows the splitting of the spots, as indicated by arrows. It also confirms the coexistence of two phases. The areal population of the R-like phase is about 50%. These findings are significantly different from the previous report where the R-like phase appears only for film thickness higher than 35 nm as deduced from AFM and second harmonic generation results for biaxial clamped thin films.[1]

In fact, similar contradictions between TEM and XRD-RSM results were observed in *all* BFO films of different thicknesses below 35 nm, on LAO single crystal substrates. Figure 3 shows cross-sectional images of BFO thin films on LAO substrate with thickness of ~24 nm (a) and ~30 nm (b). In the inset of Fig. 3(a), the SAED pattern shows spots split, indicating the coexistence of the two phases in the 24 nm film, which also confirmed by HRTEM images. The R-like phase also appears in a 30 nm film (Fig. 3(b)). For thin films thicker than 35 nm, e.g., 80 nm, the coexistence of the two phases was also observed, as shown in Fig. 3(c). However, the areal fraction of the R-like phase is estimated to be ~65%, which is much more than ~22% estimated from AFM images.

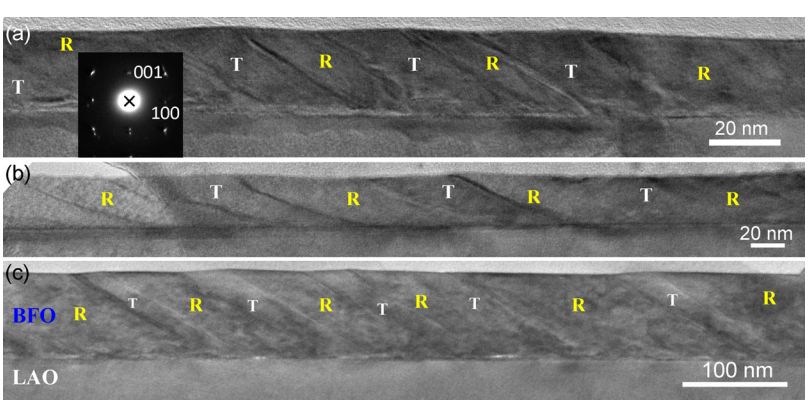

FIG. 3. (Color online) Cross-sectional TEM images of BFO thin films on LAO with thickness of ~24 nm (a), ~30 nm (b), and ~80 nm (c). Inset: [010] zone axis SAED pattern from the film containing R-like and T-like phases. It was indexed on the basis of the pseudo-cubic unit cell. The splitting of the spots indicates the coexistence of the T-like and R-like phases.

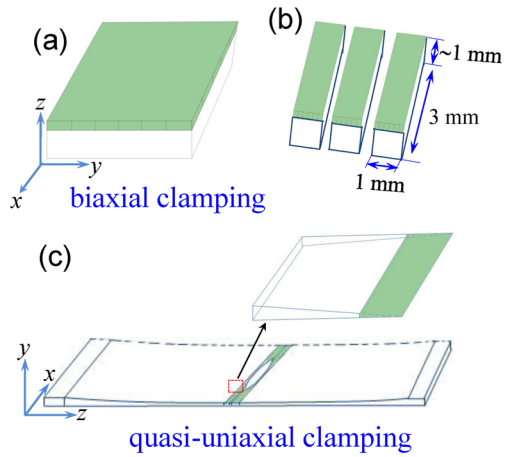

FIG. 4. (Color online) Schematics of the as-grown biaxial clamping film (a), and cut to small pieces for TEM specimens preparation (b) and part of the quasi-uniaxial clamping TEM specimen after being ground, polished, and milled (c), the marked area was enlarged.

Note that thermally activated phase transformation during specimen preparation is unlikely. Even it has been reported that the surface temperature of a specimen during ion milling may reach to 200∼400 °C under normal milling conditions.[10] Our TEM specimens were milled using PIPS (model 691, Gatan) with a low incident ion angle of 5° and a low accelerating voltage of 3 kV on a liquid N_2 cooled stage. Under these conditions, the temperature of specimen would not have reached such high.

Mechanical boundary conditions and misfit strain are known to cause crystal and domain structure changes in epitaxial thin films.[2,9,11,12] Reports in the literature show that the piezoelectric responses of a discrete $PbZr_{0.2}Ti_{0.8}O_3$ islands[13–15] produced by focus ion beam (FIB) are quite different from those of the continuous thin films clamped by the substrate. Producing a cross-sectional TEM specimen from a thin film-on-substrate sample would reduce the biaxial constraint that exists in the original sample to a quasi-uniaxial one, which will change the stress status of the film dramatically, as demonstrated by the schematics in Fig. 4. The observed effect of changing constraint on stability of the two phase state in BFO films can be considered as that of the elastic heterophase domains. According to the theory of elastic heterophase domains,[16] the stability of the two phase state is determined by the difference of the energies of indirect interaction mediated by the substrate and energy of direct interaction through the domain interfaces. In the biaxial clamping case (Fig. 4(a)), the stress state which determines indirect interaction through the substrate is biaxial stress in the plane of the film, while the stress state which determines direct interaction is uniaxial in plane of the domain interface.[16,17] The effective direct interaction increases with decreasing film thickness and makes the two phase state unstable in common biaxial constrained films on substrates. This has been proved in 80 nm- and 10 nm-thick BFO films clamped by biaxial constraint (Fig. 1). As the biaxial clamping film was cut, ground, polished, milled, and finally formed the TEM specimen, as shown in Fig. 4(c), the stress between the film and substrate changes from biaxial to uniaxial and the long range stress in the domain interface is diminished and it makes two phase state stable.

In summary, the strain induced nanoscale periodic phase separation under uniaxial and biaxial strains was studied in BFO thin films. The R-like phase due to stress status change appears even in a 12 nm-thick quasi-uniaxial constrained TEM specimen, which is quite different with the case for biaxial constraint thin films clamped by the substrate. The phase separation of BFO films is highly sensitive to the dimension of constraint strain between a thin film and a substrate.

LC acknowledges MoE RG 21/07 and ARC 16/08, MINDEF-NTU-JPP 10/12, NRF CREATE HUJ-BGU-NTU and ERI@N. YQW thanks the financial support from the National Natural Science Foundation of China (Grant No. 10974105) and the Taishan Outstanding Overseas Scholar Program of Shandong Province. ZLL thanks the support from the Natural Science Foundation of China (11004178) and the Ministry of Science and Technology of China (2010CB934501).

[1]R. J. Zeches, M. D. Rossell, J. X. Zhang, A. J. Hatt, Q. He, C. H. Yang, A. Kumar, C. H. Wang, A. Melville, C. Adamo, *et al.*, Science **326**, 977 (2009).
[2]H. Ma, L. Chen, J. L. Wang, J. Ma, and F. Boey, Appl. Phys. Lett. **92**, 182902 (2008).
[3]J. X. Zhang, B. Xiang, Q. He, J. Seidel, R. J. Zeches, P. Yu, S. Y. Yang, C. H. Wang, Y.-H. Chu, L. W. Martin, A. M. Minor, and R. Ramesh, Nat. Nanotech. **6**, 98 (2011).
[4]Z. H. Chen, L. You, C. W. Huang, Y. J. Qi, J. L. Wang, T. Sritharan, and L. Chen, Appl. Phys. Lett. **96**, 252903 (2010).
[5]Z. H. Chen, Z. L. Luo, Y. J. Qi, P. Yang, S. X. Wu, C. W. Huang, T. Wu, J. L. Wang, C. Gao, T. Sritharan, and L. Chen, Appl. Phys. Lett. **97**, 242903 (2010).
[6]Z. H. Chen, Z. L. Luo, C. W. Huang, Y. J. Qi, P. Yang, L. You, C. S. Hu, T. Wu, J. L. Wang, C. Gao, T. Sritharan, and L. Chen, Adv. Funct. Mater. **21**, 133 (2011).
[7]V. M. Kaganer, B. Jenichen, F. Schippan, W. Braun, L. Däweritz, and K. H. Ploog, Phys. Rev. Lett. **85**, 341 (2000).
[8]J. Wu, Q. Gu, B. S. Guiton, N. P. de Leon, L. Ouyang, and H. Park, Nano Lett. **6**, 2313 (2006).
[9]A. L. Roytburd and J. Slutsker, J. Mech. Phys. Solids **47**, 2299 (1999).
[10]M. J. Kim and R. W. Carpenter, Ultramicroscopy **21**, 327 (1987).
[11]N. A. Pertsev, A. G. Zembilgotov, and A. K. Tagantsev, Phys. Rev. Lett. **80**, 1988 (1998).
[12]C. W. Huang, Y. H. Chu, Z. H. Chen, J. L. Wang, T. Sritharan, Q. He, R. Ramesh, and L. Chen, Appl. Phys. Lett. **97**, 152901 (2010).
[13]V. Nagarajan, A. Roytburd, A. Stanishevsky, S. Prasertchoung, T. Zhao, L. Chen, J. Melngailis, O. Auciello, and R. Ramesh, Nat. Mater. **2**, 43 (2003).
[14]L. Chen, J. H. Li, J. Slutsker, J. Ouyang, and A. L. Roytburd, J. Mater. Res. **19**, 2853 (2004).
[15]Z. K. Ma, F. Zavaliche, L. Chen, J. Ouyang, J. Melngailis, A. L. Roytburd, V. Vaithyanathan, D. G. Schlom, T. Zhao, and R. Ramesh, Appl. Phys. Lett. **87**, 072907 (2005).
[16]A. L. Roytburd, J. Appl. Phys. **83**, 228 (1998).
[17]J. Ouyang, W. Zhang, X. Y. Huang, and A. L. Roytburd, Acta Mater. **59**, 3799 (2011).